International Journal of Control, Automation and Systems 17(1) (2019) 212-224
http://dx.doi.org/10.1007/s12555-018-0005-1
ISSN:1598-6446 eISSN:2005-4092
http://www.springer.com/12555

Circumnavigation of a Moving Target in 3D by Multi-agent Systems with Collision Avoidance: An Orthogonal Vector Fields-based Approach

Hang Zhong, Yaonan Wang, Zhiqiang Miao*, Jianhao Tan, Ling Li, Hui Zhang, and Rafael Fierro

Abstract: The problem of circumnavigating a moving target in a three dimensional setting by a network of agents while avoiding inter-agent collisions is addressed in this paper. A distributed control strategy is proposed for the multi-agent system to achieve three objectives: reaching the target plane with predesigned orientation, circulating around the target with prescribed radius, and avoiding collisions among agents. After representing the control objectives by three potential functions, the gradient fields of which are orthogonal to each other, the control law then is developed using the gradient vector field-based approach. The novelty of the proposed controller lies in the orthogonality of the vector fields, which decouples the control objectives and ensures global asymptotic convergence to the desired motion, subject to some mild initial condition constraints. The stability and convergence analysis are presented using Lyapunov tools, and the effectiveness of the proposed control strategy is demonstrated through numerical simulations.

Keywords: Circumnavigation, collision avoidance, multi-agent systems, potential function, target tracking/enclosing, vector fields.

1. INTRODUCTION

The past decade, there has been a growing research interest in the distributed coordination and cooperative control of the multi-agent system(MAS) [1–12]. Compared with a single agent, MAS provides increased efficiency, scalability, and robustness. In multi-robot coordination, one of the fundamental problems is the formation control, in which MAS aims to maintain a prescribed geometric pattern. The formation control problem can be classified as position-based control [13–15], distance-based control [16–30], and bearing-based control [31–33], depending on what relative quantity is used for specifying the desired geometric pattern. In position-based control, the desired geometric pattern is specified by relative positions among agents, and agents actively control relative positions. After an appropriate coordinate transformation, the position-based formation control problem can be reduced to a consensus problem. Hence, linear protocols can be developed to achieve global asymptotic convergence of the desired formation. On the other hand, in distance-based control or bearing-based control, agents actively control inter-agent distances or bearings. Due to the inherent nonlinearity of distance and bearing, nonlinear feedback control laws have been proposed, and the associated stability analysis relies on the concept of graph distance rigidity [20] or bearing rigidity [33].

Recently, considerable research efforts have been devoted to the development of distributed control strategies to achieve circular or enclosing formation of MAS. This is motivated by various civil and military applications like monitoring, surveillance, sampling and mapping of unknown or partially unknown environment by mobile sensor networks [34–37]. The MAS is more suitable for sensing the environment than an individual robot because it can gather multiple simultaneous measurements over a large area. In [38–44], some strategies were proposed for MAS to achieve the collective circular motion. The center of the circular formation is determined by all the initial states of MAS, thus it cannot be pre-specified. However, in some applications, MAS is expected to circle around certain specific target or area. In these target-involved missions, the goal is to circumnavigate a target of interest with specific radius by a network of autonomous agents.

Manuscript received January 3, 2018; revised June 12, 2018; accepted August 12, 2018. Recommended by Associate Editor Hyo-Sung Ahn under the direction of Editor Euntai Kim. This work was supported by the National Natural Science Foundation of China (61433016, 61573134, 61733004, 61401046), National Science and Technology Support Project (NO.2015BAF11B01), Hunan Key Laboratory of Intelligent Robot Technology in Electronic Manufacturing (NO IRF 2018009) and also funded by the Fundamental Research Funds for the Central Universities.

Hang Zhong, Yaonan Wang, Zhiqiang Miao, and Jianhao Tan are with the College of Electrical and Information Engineering, Hunan University, Changsha 410082, China (e-mails: zhonghang@hnu.edu.cn, yaonan@hnu.edu.cn; miaozhiqiang@hnu.edu.cn, tanjianhao96@sina.com). Ling Li and Hui Zhang are with the College of Electrical and Information Engineering, Changsha University of Science and Technology, Changsha 410114, China (e-mails: lanling1207@csust.edu.cn, zhanghuihby@126.com). Rafael Fierro is with MARHES Lab, Department of Electrical and Computer Engineering, University of New Mexico, Albuquerque, New Mexico 87131-0001, USA (e-mail: rfierro@unm.edu). *Corresponding author.

This problem will be referred as the circumnavigation problem, which has been studied in [45] and [46] for a single agent, and some related topics are collective circular motion with a beacon or virtual leader in [47–52], and standoff tracking of target in [53–55].

Among the abundant literature on the circumnavigation problem, the approaches to address this problem can be mainly classified as the self-propelled particles-based approach [47–52], vector field-based approach [53–56], and cyclic pursuit-based approach [57–59]. In the self-propelled particles-based approach, each agent is modeled as a Newtonian particle that moves at a constant speed subject to steering controls. The case where agents move in plane was studied in [47–50] and [51], [52] for the 3D case. Under the assumption that the target is stationary, asymptotic convergence to the desired formation can be guaranteed. However, if the target is moving, it can be shown that it is impossible for agents with constant linear velocities to asymptotically circumnavigate the moving target. In the vector field-based approach, the essential idea is constructing a vector field to globally attract agents to a limit cycle around the target. This approach stems from the artificial potential field work in mobile robotics, in the sense that the vector field can be created by adding circulation to the gradient field of a potential function, so that it would produce circular motions instead of ultimately stationary behaviors. In [53], General techniques for constructing Lyapunov vector fields that generate circular pattern attractors in 3D were developed for a single unmanned aircraft. In [54], Lyapunov guidance vector fields were utilized for two unmanned aircrafts to standoff tracking a moving target with constant speed. In [53], a guidance law was proposed to tracking a moving target with multiple aircrafts in leader-follower formation. In [56], a method for computation of artificial vector fields that enable a robot to converge to and circulate around generic time-varying curves specified in n dimensional spaces was proposed. The vector field-based approach is attractive due to its simplicity, ease of implementation, and robustness to external disturbances. However, the aforementioned studies on the applications of vector field-based approach to the circumnavigation problem focus more on one single agent, except for some simple multi-agent system cases like two-robot system and robots in the leader-follower formation. In the cyclic pursuit-based approach, n identical agents are ordered such that agent i pursues agent $i+1$ (modulo n) to form a directed ring interaction topology. In [57], a methodology based on cyclic pursuit strategy was proposed for group coordination and cooperative control of n agents to achieve a target-capturing task in 3D space. In [58], cyclic pursuit control laws were developed for spacecrafts in three dimensions to achieve a circular formation with fixed center. In [59], a control framework for achieving encirclement of a target moving in 3D with MAS was presented based on a generalized cyclic pursuit strategy, where agent i pursues agents $i-1$ and $i+1$ (modulo n) to form a undirected ring structure. The cyclic pursuit strategy inherently is decentralized and requires a small number of communication links. However, the strategy requires agents to be ordered, which is not a common setting in many engineering applications.

The vector field-based approach was extended to solve the circumnavigation problem in 3D with MAS in our paper [60]. A distributed control strategy was proposed for the robots to achieve a circular formation with prescribed radius and inter-agent distances around a moving target. Following the work in [60], here we take into account the collision avoidance issues, and consider the problem of circumnavigating a moving target in 3D with a network of agents while avoiding inter-agent collisions. The goal for the MAS is to achieve three objectives: reaching the target plane with predesigned orientation, circulating around the target with prescribed radius, and avoiding collisions among agents. The proposed vector field-based controller is easy to implement, and robust to external disturbances. The communication topology of agents is distance-based and time-varying, without the requirement of ring structure as in the cyclic pursuit strategy. The target can be stationary or moving with variable speed in 3D environments. Due to the orthogonality of the vector fields, the stability and convergence of the closed-loop system are guaranteed under some mild initial condition constraints.

The remainder of this paper is organized as follows: In Section 2, some mathematical preliminaries first are presented. Problem is formulated in Section 3. In Section 4, a control law based on three orthogonal gradient fields is proposed and main results is stated. Simulation results for illustrating the effectiveness of the proposed strategy are presented in Section 5. Section 6 concludes the paper.

The standard notations are used throughout this paper. $\mathbb{R}$ denotes the sets of real numbers, and $\mathbb{R}^n$ is the set of n-tuples for which all components belong to $\mathbb{R}$. For vector $x \in \mathbb{R}^n$, $\|x\|$ is the Euclidian 2-norm of x. Let $I_n \in \mathbb{R}^{n\times n}$ be the n-dimensional identity matrix. For matrix $A \in \mathbb{R}^{m\times n}$, denote $A^T \in \mathbb{R}^{n\times m}$ as the transpose of A. For the convenience of the reader, the main symbols to be used in this paper are summarized in Table 1.

2. MATHEMATICAL PRELIMINARIES

2.1. Multivariable calculus and vector analysis

In this subsection, some elements and results on multivariable calculus and vector analysis that will be used in the subsequent development are presented. These materials are mainly based on the formulations in [61, 62].

First, the definition and some useful properties on the derivative of vector functions, orthogonal projection matrix and cross product are introduced.

Definition 1: Let $f(x) = [f_1(x), f_2(x), \ldots, f_m(x)]^T \in$

Table 1. Main symbols used in the paper.

Symbol	Interpretation
$(\partial f/\partial x) \in \mathbb{R}^{m\times n}$	derivative of $f(x) \in \mathbb{R}^m$ to $x \in \mathbb{R}^n$
$\nabla_x f \in \mathbb{R}^n$	gradient of $f(x) \in \mathbb{R}$ to $x \in \mathbb{R}^n$
$\varphi_x \in \mathbb{R}^n$	bearing of vector $x \in \mathbb{R}^n$
$P_x \in \mathbb{R}^{n\times n}$	orthogonal projection matrix of $x \in \mathbb{R}^n$
$(a\times b) \in \mathbb{R}^3$	cross product of $a,b \in \mathbb{R}^3$
$\Omega(a) \in \mathbb{R}^{3\times 3}$	skew symmetric matrix associated with $a \in \mathbb{R}^3$
$p_i \in \mathbb{R}^3$	position of robot i
$u_i \in \mathbb{R}^3$	control input of robot i
$p_t \in \mathbb{R}^3$	position of target
$u_t \in \mathbb{R}^3$	velocity of target
$\alpha \in \mathbb{R}^3$	orientation of the target plane
$\rho > 0$	prescribed distance between the robot and target
$\delta_0 > 0$	minimum distance between robots

$\mathbb{R}^m$ be a differentiable vector function depending on $x = [x_1, x_2, \ldots, x_n]^T \in \mathbb{R}^n$, then the derivative of $f(x)$ with respect to x is defined as

$$\frac{\partial f}{\partial x} = \begin{bmatrix} \frac{\partial f_1}{\partial x_1} & \frac{\partial f_1}{\partial x_2} & \cdots & \frac{\partial f_1}{\partial x_n} \\ \frac{\partial f_2}{\partial x_1} & \frac{\partial f_2}{\partial x_2} & \cdots & \frac{\partial f_2}{\partial x_n} \\ \vdots & \vdots & \ddots & \vdots \\ \frac{\partial f_m}{\partial x_1} & \frac{\partial f_m}{\partial x_2} & \cdots & \frac{\partial f_m}{\partial x_n} \end{bmatrix}_{m\times n}. \tag{1}$$

Specifically, if $f(x) \in \mathbb{R}$ is a scalar function, then $(\partial f/\partial x)$ is a row vector. Later we may use the gradient vector $\nabla_x f = (\partial f/\partial x)^T$ to transform it into a column vector.

Property 1: Given any constant matrix $A \in \mathbb{R}^{m\times n}$, if $\|Ax\| \neq 0$, then

$$\frac{\partial (Ax/\|Ax\|)}{\partial x} = \frac{1}{\|Ax\|}(I - \frac{Axx^TA^T}{\|Ax\|^2})A. \tag{2}$$

Definition 2: Given any nonzero vector $x \in \mathbb{R}^n$, the bearing of vector x is denoted as $\varphi_x = x/\|x\|$, and the associated orthogonal projection matrix is given by

$$P_x = I - \varphi_x \varphi_x^T, \tag{3}$$

where I is the identity matrix with appropriate dimensions.

Property 2: For any nonzero vector x, the orthogonal projection matrix P_x satisfies

$$P_x x = 0;\ P_x^T = P_x;\ P_x^2 = P_x. \tag{4}$$

Moreover, matrix P_x is positive semi-definite with eigenvalues $\{0, 1, 1 \ldots, 1\}$.

Definition 3: For any two vectors $a = [a_1, a_2, a_3]^T \in \mathbb{R}^3, b = [b_1, b_2, b_3]^T \in \mathbb{R}^3$, the cross product of a and b is the vector

$$a \times b = \begin{bmatrix} a_2b_3 - a_3b_2 \\ a_3b_1 - a_1b_3 \\ a_1b_2 - a_2b_1 \end{bmatrix}, \tag{5}$$

or equivalently,

$$a \times b = \Omega(a)b, \tag{6}$$

where the associated skew symmetric matrix $\Omega(a)$ is defined as

$$\Omega(a) = \begin{bmatrix} 0 & -a_3 & a_2 \\ a_3 & 0 & -a_1 \\ -a_2 & a_1 & 0 \end{bmatrix}. \tag{7}$$

Property 3: The vector $a \times b$ is orthogonal to both a and b, i.e., $(a\times b)^T a = (a\times b)^T b = 0$; and the magnitude of the cross product $a \times b$ satisfies

$$\|a \times b\|^2 = \|a\|^2\|b\|^2 - \|a^T b\|^2. \tag{8}$$

Based on the above results, some significant connections among bearing of vectors, orthogonal projection matrix and cross product now are established.

Property 4: For any two nonzero vectors a and b, we have

$$\Omega(\varphi_a)\Omega(\varphi_b) = \varphi_b\varphi_a^T - \varphi_a^T\varphi_b. \tag{9}$$

Specifically, if $a = b$, then

$$\Omega(\varphi_a)\Omega(\varphi_a) = -P_a. \tag{10}$$

If $a^T b = 0$, then

$$\Omega(\varphi_a)\Omega(\varphi_b) = \varphi_b\varphi_a^T. \tag{11}$$

Proof: Using equation (6), we have

$$\begin{aligned} \|\varphi_a \times \varphi_b\|^2 =& -(\varphi_a \times \varphi_b)^T(\varphi_b \times \varphi_a) \\ =& -(\Omega(\varphi_a)\varphi_b)^T\Omega(\varphi_b)\varphi_a \\ =& \varphi_b^T\Omega(\varphi_a)\Omega(\varphi_b)\varphi_a. \end{aligned} \tag{12}$$

On the other hand, using Property 3, we have

$$\begin{aligned} \|\varphi_a \times \varphi_b\|^2 =& \|\varphi_a\|^2\|\varphi_b\|^2 - \|\varphi_a^T\varphi_b\|^2 \\ =& \varphi_b^T\varphi_b\varphi_a^T\varphi_a - \varphi_b^T(\varphi_a^T\varphi_b)\varphi_a \\ =& \varphi_b^T(\varphi_b\varphi_a^T - \varphi_a^T\varphi_b)\varphi_a. \end{aligned} \tag{13}$$

Equations (12) and (13) imply equation (9) holds, which subsequently yields (10) when $a = b$, and (11) when $a^T b = 0$. □

Property 5: For any two nonzero vectors a and b, if a and b are orthogonal, i.e., $a^T b = 0$, then

$$(\varphi_a \times \varphi_b)(\varphi_a \times \varphi_b)^T = P_a P_b. \tag{14}$$

Proof: Using (6), we have

$$\begin{aligned}(\varphi_a\times\varphi_b)(\varphi_a\times\varphi_b)^T &= -(\varphi_a\times\varphi_b)(\varphi_b\times\varphi_a)^T\\ &= -\Omega(\varphi_a)\varphi_b(\Omega(\varphi_b)\varphi_a)^T\\ &= \Omega(\varphi_a)\varphi_b\varphi_a^T\Omega(\varphi_b). \end{aligned}\tag{15}$$

Following equations (10) and (11), we have

$$\begin{aligned}P_aP_b &= \Omega(\varphi_a)\Omega(\varphi_a)\Omega(\varphi_b)\Omega(\varphi_b)\\ &= \Omega(\varphi_a)\varphi_b\varphi_a^T\Omega(\varphi_b).\end{aligned}\tag{16}$$

Equations (15) and (16) imply (14) holds. □

Property 6: Given two nonzero vectors $a,x\in\mathbb{R}^3$, denote $\varphi_x^a=\frac{P_ax}{\|P_ax\|}$, where $P_a=I-\varphi_a\varphi_a^T,\varphi_a=a/\|a\|$. If $\|P_ax\|\neq 0$, then

$$\frac{\partial(\varphi_x^a)}{\partial x}=\frac{1}{\|P_ax\|}(\varphi_x^a\times\varphi_a)(\varphi_x^a\times\varphi_a)^T.\tag{17}$$

Proof: Using the Properties 1 and 5 with the fact $\varphi_a^T\varphi_x^a=0$, the derivative of φ_x^a with respect to x gives

$$\begin{aligned}\frac{\partial(\varphi_x^a)}{\partial x} &= \frac{1}{\|P_ax\|}P_x^aP_a\\ &= \frac{1}{\|P_ax\|}(\varphi_x^a\times\varphi_a)(\varphi_x^a\times\varphi_a)^T,\end{aligned}\tag{18}$$

where $P_x^a=I-\varphi_x^a(\varphi_x^a)^T$ is the associated orthogonal projection matrix with φ_x^a. □

2.2. Algebraic graph theory

Information exchange between agents can be represented as a graph. Let $\mathcal{G}=\{\mathcal{V},\mathcal{E}\}$ be a digraph with a node set $\mathcal{V}=\{1,2,\ldots,n\}$, an edge set $\mathcal{E}\subseteq\mathcal{V}\times\mathcal{V}$. A directed edge denoted by (i,j) means that node i has access to node j, i.e., node i can receive information from node j. The adjacency matrix $A=[a_{ij}]_{n\times n}$ of the graph is defined as follows: If there is a directed link from node j to i ($j\neq i$), then $a_{ij}>0$; otherwise, $a_{ij}=0$. We assume that $a_{ii}=0$ for all i. A graph is called undirected if $a_{ij}>0$ implies $a_{ji}>0$ for all $i,j\in\mathcal{V}$. On the other hand, if $a_{ij}=a_{ji}$ for all $i,j\in\mathcal{V}$, then the weights are called symmetric. Clearly, if a graph has symmetric weights, then it is also undirected. The neighbor set of agent i is defined as $N_i=\{j\in\mathcal{V}\mid(i,j)\in\mathcal{E}\}$, which in the case of undirected graphs results in a mutual adjacency relationship between nodes, i.e., $i\in N_j\Longleftrightarrow j\in N_i$.

3. PROBLEM FORMULATION

Consider a multi-agent system that consists of n agents moving in a 3D space with dynamics given by

$$\dot{p}_i=u_i,\ i\in N=\{1,2,\ldots,n\},\tag{19}$$

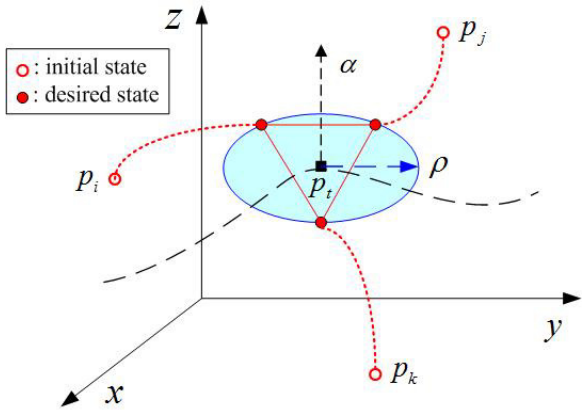

Fig. 1. Circumnavigation problem in MAS.

where $p_i\in\mathbb{R}^3$ and $u_i\in\mathbb{R}^3$ are respectively the state and control input for agent i. It is assumed that each agent is equipped with a range sensor and wireless communication capabilities. The agent can sense and communicate with other agents within a distance $d>0$. Thus, the communication neighbor for each agent i is defined as

$$N_i=\{j\in N,\ j\neq i\mid\|p_i-p_j\|\leq d\}.\tag{20}$$

The inter-agent communications can be represented as a undirected graph $G=\{V,E\}$, which consists of a set of vertices $V=\{1,2,\ldots,n\}$ indexed by the group members, and a set of edges $E=\{(i,j)\in V\times V\mid j\in N_i\}$ representing inter-agent communications.

Given a moving target with position $p_t\in\mathbb{R}^3$, and velocity $\dot{p}_t=u_t$, we assume that the position and velocity of the target are known to each agent. Although this assumption seems strong, in practice, filtering techniques can be used to estimate the state of the target at each sampled time (see for instance [45] and [46]). Here we focus on the control problem, and the estimation of the target's state is not within the scope of this paper. The control problem for the MRS considered here is to circumnavigate the moving target p_t while avoiding inter-robot collisions. The circumnavigation task requires that the robots circulate around the target with prescribed radius and within the same target plane passing through p_t, whose orientation is pre-assigned, as shown in Fig. 1. Specifically, the goal is to design a distributed control law such that the agent team

1) Reach the target plane:

$$\lim_{t\to\infty}\alpha^T(p_t-p_i)=0,\ \forall i\in N,\tag{21}$$

where $\alpha\in\mathbb{R}^3$ is a constant vector which represents the orientation of the target plane and satisfies $\|\alpha\|=1$.

2) Circulate around the target with prescribed radius:

$$\lim_{t\to\infty}\|p_t-p_i\|=\rho,\ \forall i\in N,\tag{22}$$

where $\rho > 0$ is the desired distance between agent and target.

3) Avoid inter-agent collisions:

$$\|p_i(t) - p_j(t)\| > \delta_0,\ \forall i \in N, j \in N_i, t \geq 0, \quad (23)$$

where $0 < \delta_0 < d$ is the minimum distance between agents.

4. MAIN RESULTS

In this section, vector field-based control law for the circumnavigation task is designed, and the stability analysis of the closed-loop system is presented.

Denote $p_{it} = p_i - p_t, \varphi_i = p_{it}/\|p_{it}\|$, and define

$$\varphi_i^\alpha = \frac{P_\alpha p_{it}}{\|P_\alpha p_{it}\|} = \frac{P_\alpha \varphi_i}{\|P_\alpha \varphi_i\|}, \quad (24)$$

where $P_\alpha = I - \alpha\alpha^T$. For the three objectives presented by equations (21)-(23), consider the following potential functions

$$V_1 = \frac{1}{2}\sum_i (\alpha^T p_{it})^2, \quad (25)$$

$$V_2 = \frac{1}{2}\sum_i (\|P_\alpha p_{it}\| - \rho)^2, \quad (26)$$

$$V_3 = \frac{1}{2}\sum_i \sum_{j\in N_i} a_{ij}\xi(\|\varphi_i^\alpha - \varphi_j^\alpha\|^2), \quad (27)$$

where $a_{ij} = a_{ji} > 0$, and ξ is a scalar function which satisfies

i) ξ is smooth in $(\delta, +\infty)$;

ii) $\xi \to \infty$ whenever $\|\varphi_i^\alpha - \varphi_j^\alpha\| \to \delta$;

where $\delta > 0$ is a design parameter.

The gradients of these three functions are defined as $\nabla_i V_k = (\partial V_k/\partial p_{it})^T, k = 1,2,3$. Through some simple calculations, the gradient of functions V_1 and V_2 can be easily obtained as

$$\nabla_i V_1 = \alpha^T p_{it}\alpha, \quad (28)$$

$$\nabla_i V_2 = (\|P_\alpha p_{it}\| - \rho)\varphi_i^\alpha. \quad (29)$$

Since $\alpha^T P_\alpha = \alpha^T(I - \alpha\alpha^T) = 0$, it can be checked that $\alpha^T \varphi_i^\alpha = 0$, and hence $(\nabla_i V_1)^T \nabla_i V_2 = 0$. While for the gradient of V_3, we have the following results.

Lemma 1: The gradient $\nabla_i V_3$ can be written in the form

$$\nabla_i V_3 = \frac{1}{\|P_\alpha p_{it}\|}\sum_{j\in N_i} \gamma_{ij}(\varphi_i^\alpha, \varphi_j^\alpha)(\alpha \times \varphi_i^\alpha), \quad (30)$$

where $\gamma_{ij}(\varphi_i^\alpha, \varphi_j^\alpha)$ is a scalar function given by

$$\gamma_{ij} = a_{ij}\xi'(\|\varphi_i^\alpha - \varphi_j^\alpha\|^2)(\alpha \times \varphi_i^\alpha)^T(\varphi_i^\alpha - \varphi_j^\alpha). \quad (31)$$

Moreover, $\nabla_i V_3$ and γ_{ij} possess the following properties

a) Gradient $\nabla_i V_3$ is orthogonal to both $\nabla_i V_1$ and $\nabla_i V_2$, i.e., $(\nabla_i V_1)^T(\nabla_i V_3) = 0,\ (\nabla_i V_2)^T(\nabla_i V_3) = 0$.

b) Function γ_{ij} is anticommutative regarding i and j, i.e., $\gamma_{ij}(\varphi_i^\alpha, \varphi_j^\alpha) = -\gamma_{ji}(\varphi_j^\alpha, \varphi_i^\alpha)$.

Proof: Using the definition, the gradient of V_3 is

$$\nabla_i V_3 = (\frac{\partial V_3}{\partial p_{it}})^T = (\frac{\partial V_3}{\partial \varphi_i^\alpha}\frac{\partial \varphi_i^\alpha}{\partial p_{it}})^T = (\frac{\partial \varphi_i^\alpha}{\partial p_{it}})^T(\frac{\partial V_3}{\partial \varphi_i^\alpha})^T, \quad (32)$$

and applying Property 6, we have

$$\frac{\partial \varphi_i^\alpha}{\partial p_{it}} = \frac{1}{\|P_\alpha p_{it}\|}(\alpha \times \varphi_i^\alpha)(\alpha \times \varphi_i^\alpha)^T. \quad (33)$$

The derivative of V_3 with respect to φ_i^α gives

$$\begin{aligned}\frac{\partial V_3}{\partial \varphi_i^\alpha} &= \frac{\partial V_3}{\partial(\|\varphi_i^\alpha - \varphi_j^\alpha\|^2)}\frac{\partial(\|\varphi_i^\alpha - \varphi_j^\alpha\|^2)}{\partial \varphi_i^\alpha} \\ &= \sum_{j\in N_i} a_{ij}\frac{\partial \xi}{\partial(\|\varphi_i^\alpha - \varphi_j^\alpha\|^2)}(\varphi_i^\alpha - \varphi_j^\alpha)^T \\ &= \sum_{j\in N_i} a_{ij}\xi'(\|\varphi_i^\alpha - \varphi_j^\alpha\|^2)(\varphi_i^\alpha - \varphi_j^\alpha)^T. \end{aligned} \quad (34)$$

Then it can be easily checked that $\nabla_i V_3$ satisfies equation (30) with γ_{ij} defined by equation (31). Because in equation (30) γ_{ij} is a scalar function, then it can be obtained that $(\nabla_i V_1)^T(\nabla_i V_3) = 0,\ (\nabla_i V_2)^T(\nabla_i V_3) = 0$ using the fact that $(\alpha \times \varphi_i^\alpha)$ are orthogonal to both α and φ_i^α.

Now, we move to the second point. Since γ_{ij} satisfies equation (31), and $\alpha \times \varphi_i^\alpha = \Omega(\alpha)\varphi_i^\alpha,\ \Omega^T(\alpha) = -\Omega(\alpha)$, then γ_{ij} can be rewritten as

$$\gamma_{ij} = a_{ij}\xi'(\|\varphi_i^\alpha - \varphi_j^\alpha\|^2)(\varphi_i^\alpha)^T\Omega(\alpha)\varphi_j^\alpha, \quad (35)$$

and γ_{ji} can be presented by

$$\gamma_{ji} = a_{ji}\xi'(\|\varphi_j^\alpha - \varphi_i^\alpha\|^2)(\varphi_j^\alpha)^T\Omega(\alpha)\varphi_i^\alpha. \quad (36)$$

Because $(\varphi_i^\alpha)^T\Omega(\alpha)\varphi_j^\alpha$ is a scalar, and $\Omega(\alpha)$ is skew symmetric, $(\varphi_i^\alpha)^T\Omega(\alpha)\varphi_j^\alpha = [(\varphi_i^\alpha)^T\Omega(\alpha)\varphi_j^\alpha]^T = -(\varphi_j^\alpha)^T\Omega(\alpha)\varphi_i^\alpha$. With the facts $a_{ij} = a_{ji}$, we hence have $\gamma_{ij} = -\gamma_{ji}$. This completes the proof. □

Based on the gradient fields of V_1, V_2 and V_3, we consider the control law as

$$u_i = u_i^1 + u_i^2 + u_i^3 + u_t, \quad (37)$$

$$u_i^1 = -k_1\nabla_i V_1, \quad (38)$$

$$u_i^2 = -k_2\nabla_i V_2 + k_0\|P_\alpha p_{it}\|(\alpha \times \varphi_i^\alpha), \quad (39)$$

$$u_i^3 = -k_3\|P_\alpha p_{it}\|\nabla_i V_3, \quad (40)$$

where k_1, k_2, and k_3 are positive gains, and k_0 is a constant representing the angular velocity of the circular motion.

To facilitate the following analysis, it is assumed that the initial conditions of the MAS satisfy:

Assumption 1: There exist two positive constants ε, δ, such that for all $i, j \in N$, $\|P_\alpha p_{it}(0)\| \geq \varepsilon$, $\|\varphi_i^\alpha(0) - \varphi_j^\alpha(0)\| > \delta$, and δ satisfies $\delta \geq \delta_0 / \min\{\varepsilon, \rho\}$.
Now we are ready to state the main result:

Theorem 1: Consider the system (19) with control law (37). If the initial condition satisfies Assumption 1, then the closed-loop system is stable, and ultimately the objectives in (21)-(23) will be achieved.

Proof: The closed-loop system of (19) and (37) is

$$\dot{p}_{it} = u_i^1 + u_i^2 + u_i^3. \tag{41}$$

Take the Lyapunov function

$$V = V_1 + V_2 + V_3, \tag{42}$$

where V_1, V_2 and V_3 are defined by (25)-(27). Because $\nabla_i V_1$, $\nabla_i V_2$ and $\nabla_i V_3$ (or $\alpha \times \varphi_i^\alpha$) are orthogonal to each other, the time derivative of V_1 and V_2 along (41) can be obtained as

$$\dot{V}_1 = \sum_i (\nabla_i V_1)^T (u_i^1 + u_i^2 + u_i^3) = -k_1 \sum_i \|\nabla_i V_1\|^2, \tag{43}$$

$$\dot{V}_2 = \sum_i (\nabla_i V_2)^T (u_i^1 + u_i^2 + u_i^3) = -k_2 \sum_i \|\nabla_i V_2\|^2. \tag{44}$$

The time derivative of V_3 along (42) is

$$\begin{aligned}
\dot{V}_3 =& \sum_i (\nabla_i V_3)^T \dot{p}_{it} + \sum_j (\nabla_j V_3)^T \dot{p}_{jt} \\
=& 2\sum_i (\nabla_i V_3)^T \dot{p}_{it} \\
=& 2\sum_i (\nabla_i V_3)^T (u_i^1 + u_i^2 + u_i^3) \\
=& 2\sum_i \|P_\alpha p_{it}\| (\nabla_i V_3)^T (k_0(\alpha \times \varphi_i^\alpha) - k_3 \nabla_i V_3) \\
=& -2k_3 \sum_i \|P_\alpha p_{it}\| \|\nabla_i V_3\|^2 \\
& + 2k_0 \sum_i \|P_\alpha p_{it}\| (\nabla_i V_3)^T (\alpha \times \varphi_i^\alpha).
\end{aligned} \tag{45}$$

Substituting the expression of $\nabla_i V_3$ in equation (30) into equation (45), and using the fact $(\alpha \times \varphi_i^\alpha)^T (\alpha \times \varphi_i^\alpha) = 1$, as well as $\gamma_{ij} = -\gamma_{ji}$, we have

$$\begin{aligned}
\dot{V}_3 =& -2k_3 \sum_i \|P_\alpha p_{it}\| \|\nabla_i V_3\|^2 \\
& + 2k_0 \sum_i \sum_{j \in N_i} \gamma_{ij}(\varphi_i^\alpha, \varphi_j^\alpha)(\alpha \times \varphi_i^\alpha)^T (\alpha \times \varphi_i^\alpha) \\
=& -2k_3 \sum_i \|P_\alpha p_{it}\| \|\nabla_i V_3\|^2 + 2k_0 \sum_i \sum_{j \in N_i} \gamma_{ij} \\
=& -2k_3 \sum_i \|P_\alpha p_{it}\| \|\nabla_i V_3\|^2 \\
& + k_0 \sum_i \sum_{j \in N_i} \gamma_{ij}(\varphi_i^\alpha, \varphi_j^\alpha) + k_0 \sum_i \sum_{j \in N_i} \gamma_{ji}(\varphi_j^\alpha, \varphi_i^\alpha) \\
=& -2k_3 \sum_i \|P_\alpha p_{it}\| \|\nabla_i V_3\|^2.
\end{aligned} \tag{46}$$

Following equation (44) it can be concluded that if $\|P_\alpha p_{it}(0)\| \geq \varepsilon > \rho$, then $\|P_\alpha p_{it}(t)\|$ is decreasing with time and converge to ρ; if $\varepsilon \leq \|P_\alpha p_{it}(0)\| < \rho$, then $\|P_\alpha p_{it}(t)\|$ is increasing with time and converge to ρ. Hence we have $\|P_\alpha p_{it}(t)\| \geq \min\{\varepsilon, \rho\} > 0$, $t \geq 0$. Because $\|P_\alpha p_{it}(t)\| > 0$ for all $t \geq 0$, we have $\dot{V} \leq 0$ following equations (43), (44) and (46), which implies the closed-loop system is stable. Equations (43) and (44) also yield for all i, $\nabla_i V_1 = 0$ and $\nabla_i V_2 = 0$ when t tends to infinity, which imply $\lim_{t\to\infty} \alpha^T (p_i(t) - p_t(t)) = 0$, and $\lim_{t\to\infty} \|P_\alpha p_{it}(t)\| = \lim_{t\to\infty} \|p_{it}(t)\| = \rho$ for all i. Thus the objectives (21) and (22) are achieved.

In the following, we will show the validity of equation (23). Since $\dot{V}_3 \leq 0$, $V_3(t) \leq V_3(0) < \infty, \forall t \geq 0$; and if $\|\varphi_i^\alpha - \varphi_j^\alpha\| \to \delta$ for at least one agent pair $(i, j) \in E$, then $\xi \to \infty$ and hence $V_3 \to \infty$. It can be easily concluded that for all $i, j \in N, t \geq 0$, $\|\varphi_i^\alpha(t) - \varphi_j^\alpha(t)\| > \delta$, or

$$F(t) = \left\| \frac{P_\alpha p_{it}(t)}{\|P_\alpha p_{it}(t)\|} - \frac{P_\alpha p_{jt}(t)}{\|P_\alpha p_{jt}(t)\|} \right\| > \delta, \tag{47}$$

and the function F satisfies

$$F^2 = 2 - \frac{2 p_{it}^T P_a p_{jt}}{\|P_\alpha p_{it}\| \|P_\alpha p_{jt}\|}. \tag{48}$$

Using Property 2, we have

$$\|P_a p_{it} - P_a p_{jt}\| \leq \lambda_{max}(P_a) \|p_{it} - p_{jt}\| \leq \|p_{it} - p_{jt}\|, \tag{49}$$

where $\lambda_{max}(P_a)$ is the largest eigenvalue of P_a. This gives

$$\begin{aligned}
\|p_{it} - p_{jt}\|^2 \geq& \|P_a p_{it} - P_a p_{jt}\|^2 \\
=& \|P_a p_{it}\|^2 + \|P_a p_{jt}\|^2 - 2 p_{it}^T P_a p_{jt} \\
=& \|P_a p_{it}\|^2 + \|P_a p_{jt}\|^2 \\
& + (F^2 - 2) \|P_a p_{it}\| \|P_a p_{jt}\| \\
\geq& F^2 \|P_a p_{it}\| \|P_a p_{jt}\|,
\end{aligned} \tag{50}$$

which implies $\|p_{it} - p_{jt}\| > \delta_0$ with the fact $F^2 > \delta^2$, $\|P_\alpha p_{it}(t)\| \geq \min\{\varepsilon, \rho\} > 0$, $t \geq 0$ and $\delta \geq \delta_0 / \min\{\varepsilon, \rho\}$. This completes the proof. □

Because the convergence and collision avoidance analysis of the closed-loop system are provided with the Lyapunov method, they are robustness to external disturbances. Take the property of collision avoidance for example, the artificial potential field-based approach is utilized, which has been demonstrated to be a robust method for collision avoidance in numerous literature. If the issue of robustness is not considered, we have the following result:

Corollary 1: Theorem 1 still holds under Assumption 1 if $k_3 = 0$ in the control law (37).

Proof: When $k_3 = 0$ in the control law (37), the arguments and conclusions on $\dot{V}_1$ and $\dot{V}_2$ still hold, the convergence of (21) and (22) are guaranteed. Moreover, with the control law (37), we have for $\forall i \in N$,

$$\dot{\varphi}_i^\alpha = (k_0 - \frac{k_3}{\|P_a p_{it}\|} \sum_{j \in N_i} \gamma_{ij})(\alpha \times \varphi_i^\alpha). \tag{51}$$

If $k_3 = 0$, then $\dot{\varphi}_i^\alpha - \dot{\varphi}_j^\alpha = k_0(\alpha \times (\varphi_i^\alpha - \varphi_j^\alpha))$, $\forall i, j \in N$. Thus, $\mathrm{d}(\|\varphi_i^\alpha - \varphi_j^\alpha\|)/\mathrm{d}t = 0$, and $\|\varphi_i^\alpha(t) - \varphi_j^\alpha(t)\| = \|\varphi_i^\alpha(0) - \varphi_j^\alpha(0)\|$, $\forall t \geq 0$. Under Assumption 1, we have $\|\varphi_i^\alpha(t) - \varphi_j^\alpha(t)\| > \delta$, $\forall t \geq 0$, and which implies $\|p_{it}(t) - p_{jt}(t)\| > \delta_0$, $\forall t \geq 0$, using similar arguments in the proof Theorem 1. □

5. SIMULATION RESULTS

In this section, we carry out some numerical simulations to illustrate the validity of the proposed strategy. First a simple case is considered to show the robustness of the proposed controller by comparing the performances of the control law (37) setting $k_3 = 0$ with that setting $k_3 > 0$. In the first case, a multi-agent system of 3 agents is expected to circumnavigate a constant moving target. The initial positions of agents and target are given by

$$p_1(0) = [-1,2,0]^T \text{ m},\ p_2(0) = [1,2,-0.5]^T \text{ m},$$
$$p_3(0) = [2,2,-1]^T \text{ m},\ p_t(0) = [0,0,0]^T \text{ m}.$$

The parameters related to the control objectives are:

$$u_t = [2,0,0]^T \text{ m/s},\ \ \alpha = [1,0,0]^T,$$
$$\rho = 1 \text{ m},\ \ \delta_0 = 0.2 \text{ m}.$$

Specifically, the velocity of target to be circled is $u_t = [2,0,0]^T$ m/s; the orientation of the target plane is specified as the vertical axis, that is, $\alpha = [1,0,0]^T$. The desired radius of the circle is $\rho = 1$ m, and $\delta_0 = 0.2$ m is the minimum inter-agent distance.

In the controller implementation, the communication distance between agents is set as $d = 0.5$ m, and $a_{ij} = 1$ if $\|p_i - p_j\| \leq 0.5$, otherwise $a_{ij} = 0$. The nonlinear function $\xi = -\ln(\|\varphi_i^\alpha - \varphi_j^\alpha\|^2 - \delta^2)$ with $\delta = 0.2$. The control gains in the control law (37) are selected as $k_0 = 3, k_1 = 2, k_2 = 8$, and $k_3 = 2$ as well as $k_3 = 0$ are simulated to compare their performance. Noting that if $k_3 = 0$, the term for inter-agent collision avoidance is not incorporated in the control law, then there are no interactions among agents, and each agent moves independently. In the simulation, the multi-agent system is numerically simulated for 20 sec, and a disturbance $u_d = [0.1\sin(2t), 0.3, 0]^T$ is added to the dynamics of each agent after 10 seconds. The simulation results for control with $k_3 = 0$ and $k_3 = 2$ are shown in Fig. 2 and Fig. 3, respectively. As seen from Figs. 2(a)-2(c) and Figs. 3(a)-3(c), the objectives specified in (21) and (22) can be achieved for both $k_3 = 0$ and $k_3 = 2$, with perfect performance if there is no disturbance, and tolerable control errors if disturbance exists. However, this is not true for the collision avoidance objective presented in (23). In order to show the details, the distances between agents are draw with different scales for the first and second ten-second in Fig. 2(d) and Fig. 3(d). For $k_3 = 0$ in the first ten-second, all the inter-agent distances are greater than $\delta_0 = 0.2$, but the distance between agent pair $(2,3)$ may become less than 0.2 at some points when the disturbance is imposed, which implies the inter-agent collision would occur. While for $k_3 = 2$, the distances among agents are always greater than 0.2, even simulated with disturbance. Comparing Fig. 2(d) and Fig. 3(d), it can be concluded that inter-agent collision avoidance is ensured only when $k_3 = 2$, and it is not when $k_3 = 0$, through it does for the first ten-second. The pseudo-distance between agents $\|\varphi_i^\alpha - \varphi_j^\alpha\|$ illustrated in Fig. 2(e) and Fig. 3(e) also imply this fact, because $\|\varphi_i^\alpha - \varphi_j^\alpha\| > 0.2$ is sufficient to ensure $\|p_i - p_j\| > 0.2$, and $\|\varphi_i^\alpha - \varphi_j^\alpha\| \to \|p_i - p_j\|/\rho$ when $\|p_i - p_t\| \to \rho$ and $\alpha^T(p_i - p_t) \to 0$. In Fig. 2(e), the pseudo-distances $\|\varphi_i^\alpha - \varphi_j^\alpha\|$ for all $i \neq j$ remain unchanged for the first ten-second, however, $\|\varphi_2^\alpha - \varphi_3^\alpha\|$ fluctuates around 0.2 in the following ten-second. In Fig. 3(e), $\|\varphi_i^\alpha - \varphi_j^\alpha\| > 0.2$ for all $i \neq j$ all the time, which yields $\|p_i - p_j\| > 0.2$ for all $i \neq j$ all the time. Compared with the signals in Figs. 2(d) and 2(e), it should be noted that there are slight oscillations in the signals of Figs. 3(d) and 3(e) at the beginning of the second ten-second, which are caused by the control input oscillations at the same time shown in Fig. 3(f). The comparison results illustrated in Figs. 2 and 3 demonstrate that it is necessary to address the issue of inter-agent collision avoidance in the control design, and the proposed strategy shows robust control performance.

In the following, we consider a more complex case where 10 agents are controlled to circumnavigate a moving target with time-varying velocity. The initial positions of agents and target are given by

$$p_1(0) = [-1,3,0]^T \text{ m},\ \ p_2(0) = [-2,1,-1]^T \text{m},$$
$$p_3(0) = [-2,-0.5,-1]^T \text{ m},$$
$$p_4(0) = [-0.5,-2,-2]^T \text{ m},\ \ p_5(0) = [3,-3,1]^T \text{ m},$$
$$p_6(0) = [1,-3,0]^T \text{ m},\ \ p_7(0) = [-2,-1,1]^T \text{ m},$$
$$p_8(0) = [2,0.5,-1]^T \text{ m},\ \ p_9(0) = [0.5,2,-2]^T \text{ m},$$
$$p_{10}(0) = [-3,3,-1]^T \text{ m},\ \ p_t(0) = [0,0,0]^T \text{m}.$$

The objective-related parameters which have the same meanings as mentioned in the first case are chosen as

$$u_t = [0.5\sin(0.2t),\ 0.3\cos(0.4t),\ 0.5]^T \text{ m/s},$$
$$\alpha = [0,0,1]^T,\ \ \rho = 2 \text{ m},\ \ \delta_0 = 0.2 \text{ m}.$$

The parameters that used in the control development are

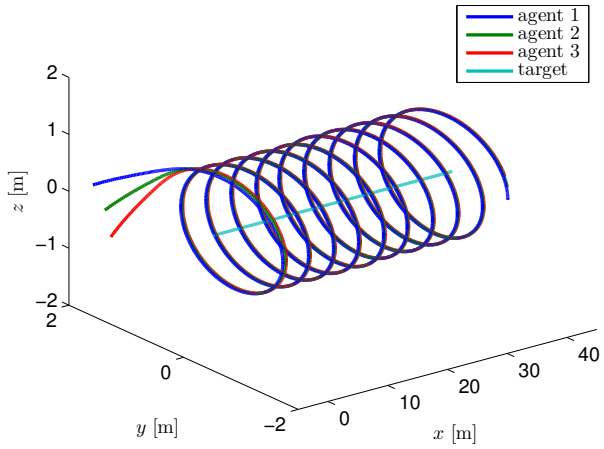

(a) Agent's trajectories in 3D.

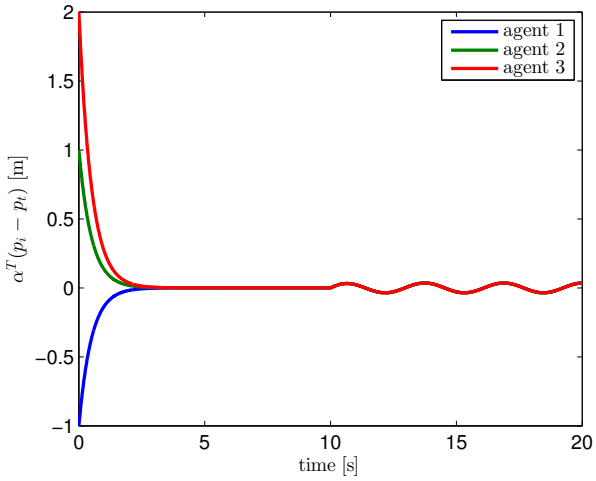

(b) Target plane convergence.

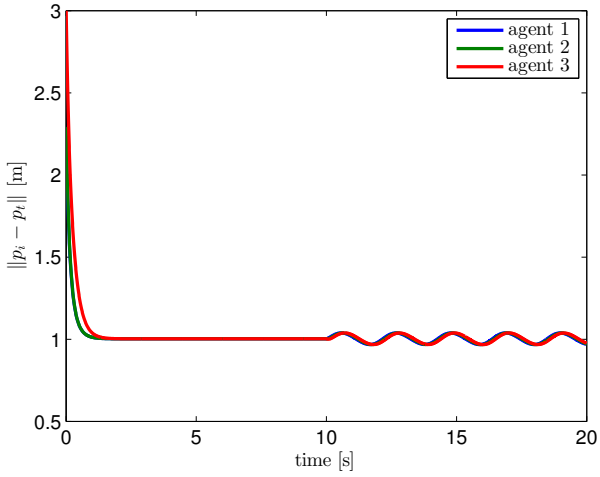

(c) Distance between agent and target $\|p_i - p_t\|$.

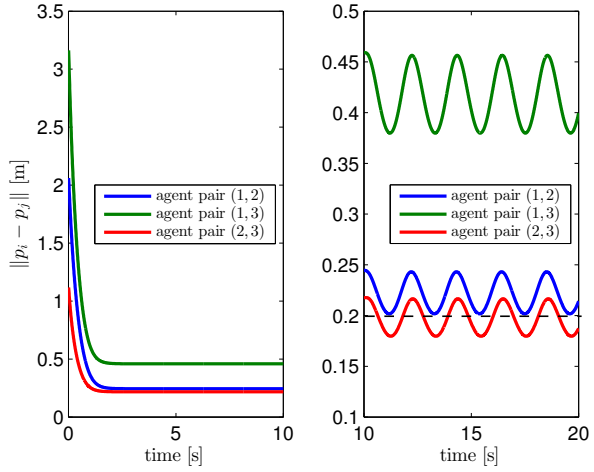

(d) Distance between agents $\|p_i - p_j\|$.

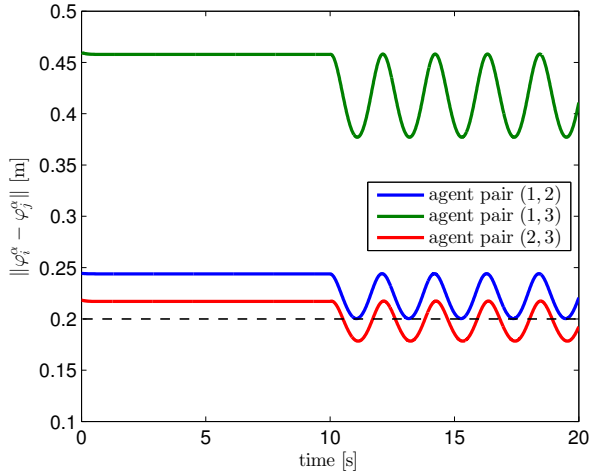

(e) Pseudo-distance between agents $\|\varphi_i^\alpha - \varphi_j^\alpha\|$.

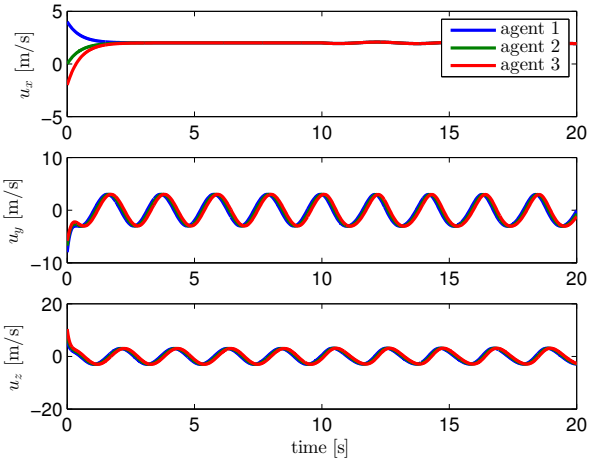

(f) Control input for agents.

Fig. 2. Simulation results for the first case with $k_3 = 0$.

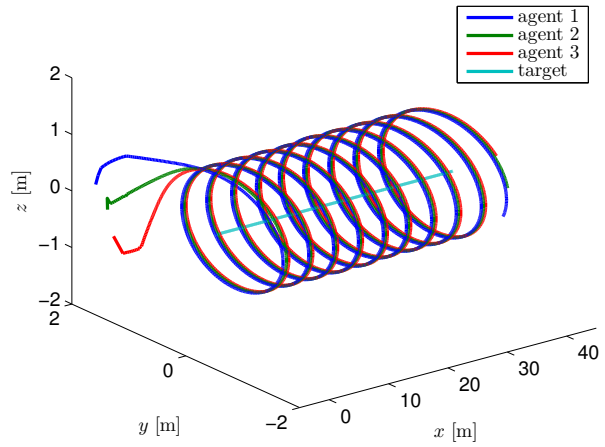

(a) Agent's trajectories in 3D.

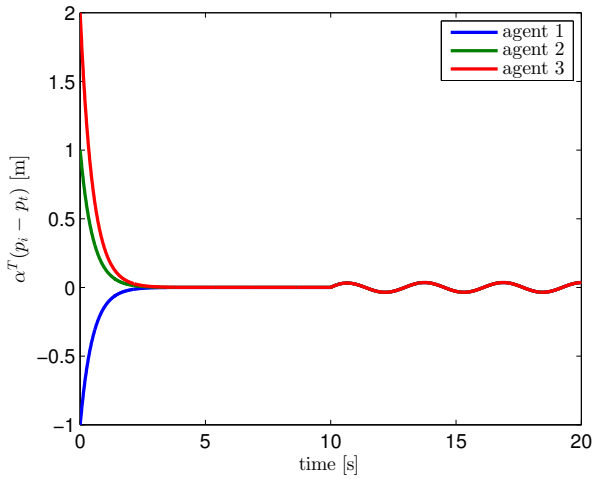

(b) Target plane convergence.

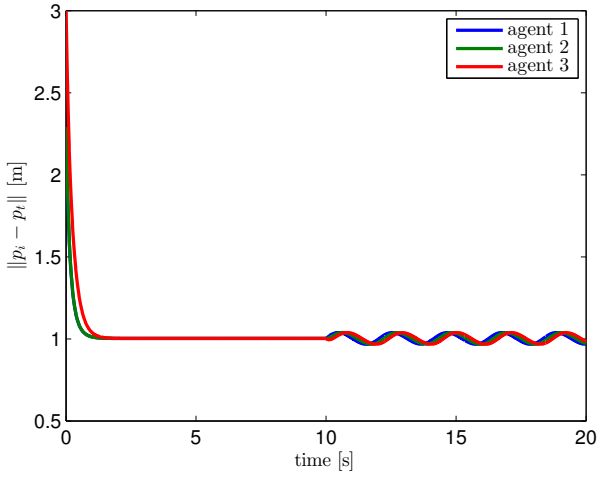

(c) Distance between agent and target $\|p_i - p_t\|$.

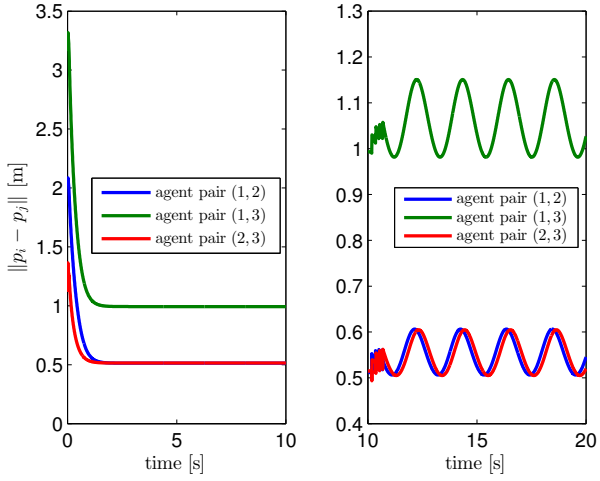

(d) Distance between agents $\|p_i - p_j\|$.

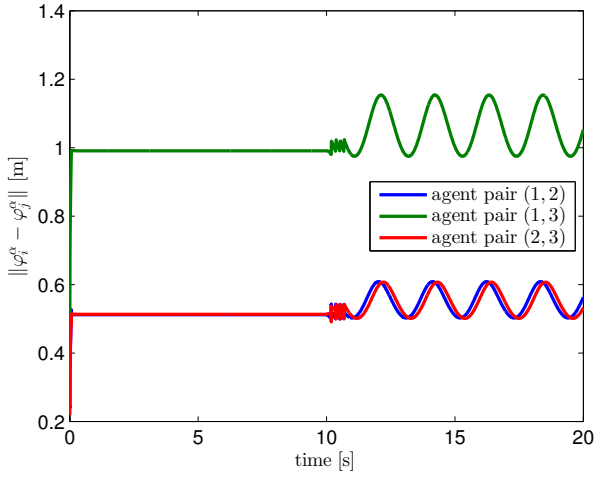

(e) Pseudo-distance between agents $\|\varphi_i^\alpha - \varphi_j^\alpha\|$.

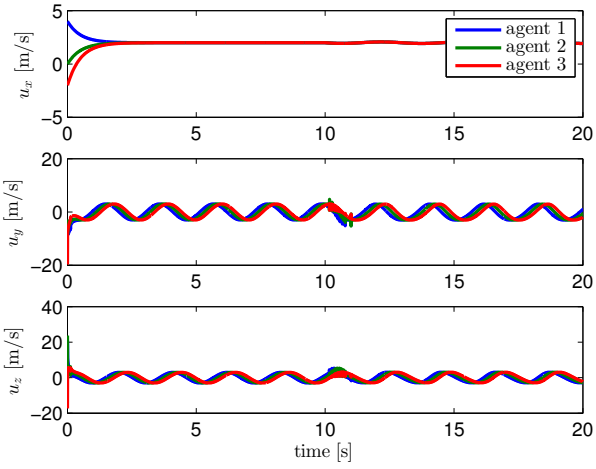

(f) Control input for agents.

Fig. 3. Simulation results for the first case with $k_3 = 2$.

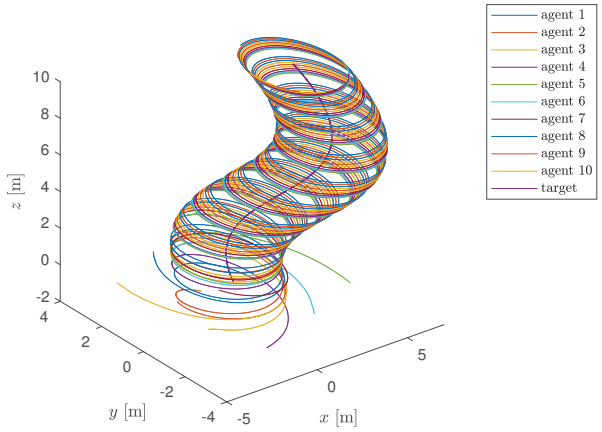

(a) Agent's trajectories in 3D.

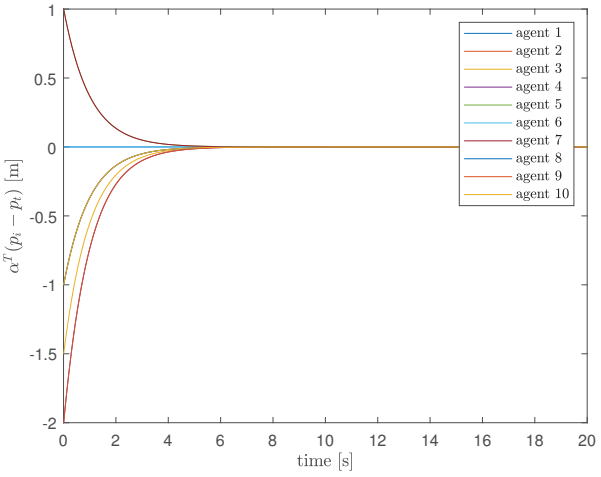

(b) Target plane convergence.

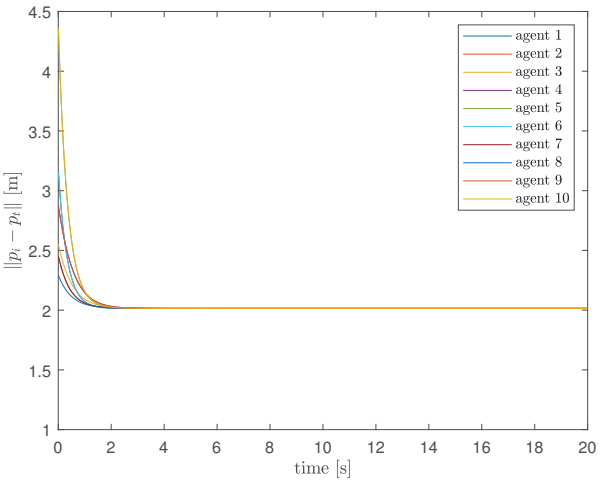

(c) Distance between agent and target $\|p_i - p_t\|$.

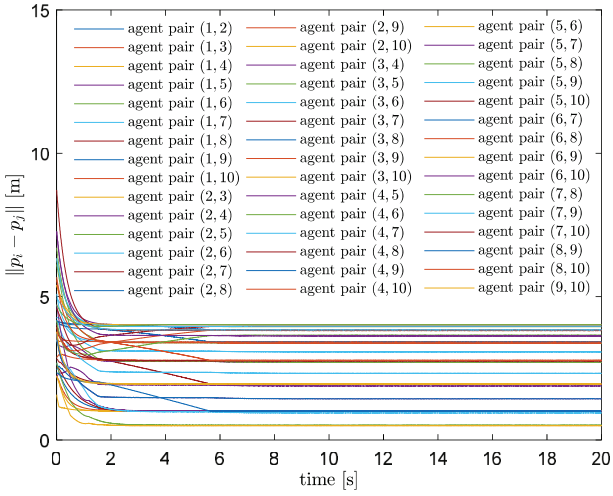

(d) Distance between agents $\|p_i - p_j\|$.

Fig. 4. Simulation results for the second case.

set as

$$d = 0.5 \text{ m}, \; a_{ij} = 1,$$
$$\xi = -\ln(\|\varphi_i^\alpha - \varphi_j^\alpha\|^2 - \delta^2), \text{ with } \delta = 0.1;$$
$$k_0 = 3, \;\; k_1 = 1, \;\; k_2 = 3, \;\; k_3 = 1.$$

Under these conditions, the simulation results for the second case are illustrated in Fig. 4. It can be observed that for all agents, $\alpha^T(p_i - p_t)$ shown in Fig. 4(b) are converge to zero; the distances between agents and target presented in Fig. 4(c) are converge to 2 m, and the inter-agent distances shown in Fig. 4(d) always great than 0.2 m. The effectiveness of the proposed control strategy thus is validated.

6. CONCLUSION

In this paper, distributed control algorithm was proposed for a multi-robot system to circumnavigate a moving target in 3D while avoiding inter-agent collisions. By exploiting the orthogonality of vector fields formulated for each of the control objectives, asymptotic convergence to the desired motion is guaranteed under some mild initial condition constraints. Formal stability and convergence analysis of the closed-loop system were presented explicitly using the Lyapunov theory. Future work may include extension of the proposed strategy to agents with double-integrator dynamics or even nonholonomic dynamics, and implementation of the proposed control law on a real multi-robot test bed to further validate the theoretic results.

REFERENCES

[1] W. Ren and R. W. Beard, *Distributed Consensus in Multi-vehicle Cooperative Control*, Springer-Verlag, London, U.K., 2008.

[2] F. Bullo, J. Cortes, and S. Martinez, *Distributed Control of Robotic Networks*, Princeton Univ., Princeton, NJ, 2009.

[3] Z. Qu, *Cooperative Control of Dynamical Systems: Applications to Autonomous Vehicles*, Springer-Verlag, London, U.K., 2009.

[4] M. Mesbahi and M. Egerstedt, *Graph Theoretic Methods for Multi-agent Networks*, Princeton Univ., Princeton, NJ, 2010.

[5] W. Ren and Y. Cao, *Distributed Coordination of Multi-Agent Networks*, Springer-Verlag, London, U.K., 2011.

[6] H. Bai, M. Arcak, and J. Wen, *Cooperative Control Design: A Systematic, Passivity-based Approach*, Springer-Verlag, New York, 2011.

[7] E. Semsar-Kazerooni and K. Khorasani, *Team Cooperation in a Network of Multi-vehicle Unmanned Systems: Synthesis of Consensus Algorithms*, Springer, New York, 2012.

[8] F. L. Lewis, H. Zhang, K. Hengster-Movric, and A. Das, *Cooperative Control of Multi-agent Systems*, Springer-Verlag, London, U.K., 2014.

[9] X. H. Wang and H. B. Ji, "Leader-follower consensus for a class of nonlinear multi-agent systems," *Int. J. Control, Automat. Syst.*, vol. 10, no. 1, pp. 27-35, 2012.

[10] Y. Cao, W. Yu, W. Ren, and G. Chen, "An overview of recent progress in the study of distributed multi-agent coordination," *IEEE Trans. Ind. Informat.*, vol. 9, no. 1, pp. 427-438, 2013.

[11] J. L. Zhang, D. L. Qi, and M. Yu, "A game theoretic approach for the distributed control of multi-agent systems under directed and time-varying topology," *IEEE Trans. Ind. Informat.*, vol. 12, no. 4, pp.749-758, 2014.

[12] K. K. Oh, M. C. Park, and H. S. Ahn, "A survey of multi-agent formation control," *Automatica*, vol. 53, pp. 424-440, 2015.

[13] J. A. Fax and R. M. Murray, "Information flow and cooperative control of vehicle formations," *IEEE Trans. Autom. Control*, vol. 49, no. 9, pp. 1465-1476, 2004.

[14] R. Olfati-Saber, J. Fax, and R. Murray, "Consensus and cooperation in networked multi-agent systems," *Proc. IEEE*, vol. 95, no. 1, pp. 215-233, Jan. 2007.

[15] K. K. Oh and H. S. Ahn, "Formation control of mobile agents based on distributed position estimation," *IEEE Trans. Autom. Control*, vol. 58, no. 3, pp. 737-742, 2013.

[16] Z. Peng, G. Wen, S. Yang, and A. Rahmani, "Distributed consensus-based formation control for nonholonomic wheeled mobile robots using adaptive neural network," *Nonlinear Dynamics*, vol. 68, no. 1, pp. 605-622, 2016.

[17] L. Asimow and B. Roth, "The rigidity of graphs," *Trans. Amer. Math. Soc.*, vol. 245, pp. 279-289, 1978.

[18] L. Asimow and B. Roth, "The rigidity of graphs, II," *J. Math. Anal. Appl.*, vol. 68, no. 1, pp. 171-190, 1979.

[19] B. Hendrickson, "Conditions for unique graph realizations," *SIAM J. Comput.*, vol. 21, no. 1, pp. 65-84, 1992.

[20] J. M. Hendrickx, B. Anderson, J. C. Delvenne, and V. D. Blondel, "Directed graphs for the analysis of rigidity and persistence in autonomous agent systems," *Int. J. Robust Nonlin.*, vol. 17, no. 10-11, pp. 960-981, 2007.

[21] C. Yu, J. M. Hendrickx, B. Fidan, B. D. Anderson, and V. D. Blondel, "Three and higher dimensional autonomous formations: Rigidity, persistence and structural persistence," *Automatica*, vol. 43, no. 3, pp. 387-402, 2007.

[22] B. Anderson, C. Yu, B. Fidan, and J. M. Hendrickx, "Rigid graph control architectures for autonomous formations," *IEEE Contr. Syst. Mag.*, vol. 28, no. 6, pp. 48-63, 2008.

[23] C. Yu, B. Anderson, S. Dasgupta, and B. Fidan, "Control of minimally persistent formations in the plane," *SIAM J. Control Optim.*, vol. 48, no. 1, pp. 206-233, 2009.

[24] D. V. Dimarogonas and K. H. Johansson, "Stability analysis for multi-agent systems using the incidence matrix: Quantized communication and formation control," *Automatica*, vol. 46, pp. 695-700, 2010.

[25] F. Dorfler and B. Francis, "Geometric analysis of the formation problem for autonomous robots," *IEEE Trans. Autom. Control*, vol. 55, no. 10, pp. 2379-2384, 2010.

[26] T. H. Summers, C. Yu, S. Dasgupta, and B. Anderson, "Control of minimally persistent leader-remote-follower and coleader formations in the plane," *IEEE Trans. Autom. Control*, vol. 56, no. 12, pp. 2778-2792, 2011.

[27] K. K. Oh and H. S. Ahn, "Formation control of mobile agents based on inter-agent distance dynamics," *Automatica*, vol. 47, no. 10, pp. 2306-2312, 2011.

[28] D. Zelazo, A. Franchi, H. H. Bulthoff, and P. Robuff, "Decentralized rigidity maintenance control with range measurements for multi-robot systems," *Int. J. Robot. Res.*, 0278364914546173, 2014.

[29] G. Wen, Z. Peng, and Y. Yu, "Planning and control of three-dimensional multi-agent formations," *IMA Journal of Mathematical Control and Information*, vol. 30, no. 2, pp. 265-284, 2012.

[30] K. K. Oh and H. S. Ahn, "Leader-follower type distance-based formation control of a group of autonomous agents," *Int. J. Control, Automat. Syst.*, vol. 15, no. 4, pp. 1738-1745, 2017.

[31] A. Franchi, C. Masone, V. Grabe, M. Ryll, H. Bulthoff, and P. Giordano, "Modeling and control of UAV bearing-formations with bilateral high-level steering," *Int. J. Robot. Res.*, 0278364912462493, 2012.

[32] S. Zhao, F. Lin, K. Peng, B. M. Chen, and T. H. Lee, "Distributed control of angle-constrained cyclic formations using bearing-only measurements," *Syst. Control Lett.*, vol. 63, pp. 12-24, Feb. 2014.

[33] S. Zhao and D. Zelazo, "Bearing rigidity and almost global bearing-only formation stabilization," *IEEE Trans. Autom. Control*, vol. 61, no.5, pp. 1255-1268, 2016.

[34] D. Paley, N. E. Leonard, R. Sepulchre, D. Grunbaum, and J. Parrish, "Oscillator models and collective motion," *IEEE Contr. Syst. Mag.*, vol. 27, no. 4, pp. 89-105, 2007.

[35] N. E. Leonard, D. Paley, F. Lekien, R. Sepulchre, D. M. Fratantoni, and R. E. Davis, "Collective motion, sensor networks, and ocean sampling," *Proc. IEEE*, vol. 95, no. 1, pp. 48-74, 2007.

[36] R. W. Beard, D. Kingston, D. Johanson, T. W. McLain, and D. B. Nelson, "Decentralized cooperative aerial surveillance using fixed-wing miniature UAVs," *Proc. IEEE*, vol. 94, no. 7, pp. 1306-1324, 2006.

[37] M. Dunbabin and L. Marques, "Robots for environmental monitoring: significant advancements and applications," *IEEE Robot Autom. Mag.*, vol. 19, no. 1, pp. 24-39, 2012.

[38] J. Marshall, M. E. Broucke, and B. Francis, "Formations of vehicles in cyclic pursuit," *IEEE Trans. Autom. Control*, vol. 49, no. 11, pp. 1963-1974, 2004.

[39] J. Marshall, M. E. Broucke, and B. Francis, "Pursuit formations of unicycles," *Automatica*, vol. 42, no. 1, pp. 3-12, 2006.

[40] W. Ding, G. Yan, and Z. Lin, "Collective motions and formations under pursuit strategies on directed acyclic graphs," *Automatica*, vol. 46, no. 1, pp. 174-181, 2010.

[41] W. Ren, "Collective motion from consensus with cartesian coordinate coupling," *IEEE Trans. Autom. Control*, vol. 54, no. 6, pp. 1330-1335, 2009.

[42] N. Moshtagh, N. Michael, A. Jadbabaie, and K. Daniilidis, "Vision-based, distributed control laws for motion coordination of nonholonomic robots," *IEEE Trans. Robot.*, vol. 25, no. 4, pp. 851-860, 2009.

[43] Z. Chen and H. T. Zhang, "No-beacon collective circular motion of jointly connected multi-agents," *Automatica*, vol. 47, no. 9, pp. 1929-1937, 2011.

[44] Z. Chen and H. T. Zhang, "A remark on collective circular motion of heterogeneous multi-agents," *Automatica*, vol. 49, no. 5, pp. 1236-1241, 2013.

[45] I. Shames, S. Dasgupta, B. Fidan, and B. Anderson, "Circumnavigation using distance measurements under slow drift," *IEEE Trans. Autom. Control*, vol. 57, no. 4, pp. 889-903, 2012.

[46] M. Deghat, I. Shames, B. D. Anderson, and C. Yu, "Localization and circumnavigation of a slowly moving target using bearing measurements," *IEEE Trans. Autom. Control*, vol. 59, no. 8, pp. 2182-2188, 2014.

[47] R. Sepulchre, D. A. Paley, and N. E. Leonard, "Stabilization of planar collective motion: all-to-all communication," *IEEE Trans. Autom. Control*, vol. 52, no. 5, pp. 811-824, 2007.

[48] R. Sepulchre, D. A. Paley, and N. E. Leonard, "Stabilization of planar collective motion with limited communication," *IEEE Trans. Autom. Control*, vol. 53, no. 3, pp. 706-719, 2008.

[49] G. S. Seyboth, J. Wu, and J. Qin, "Collective circular motion of unicycle type vehicles with non-identical constant velocities," *IEEE Trans. Contr. Netw. Syst.*, vol. 1, no. 2, pp. 167-176, 2014.

[50] N. Ceccarelli, M. Di Marco, A. Garulli, and A. Giannitrapani, "Collective circular motion of multi-vehicle systems," *Automatica*, vol. 44, no. 12, pp. 3025-3035, 2008.

[51] S. Hernandez and D. Paley, "Three-dimensional motion coordination in a spatiotemporal flow field," *IEEE Trans. Autom. Control*, vol. 55, no. 12, pp. 2805-2810, 2010.

[52] L. Scardovi, N. Leonard, and R. Sepulchre, "Stabilization of three-dimensional collective motion," *Commun. Inf. Syst.*, vol. 8, no. 4, pp. 473-500, 2008.

[53] D. A. Lawrence, E. W. Frew, and W. J. Pisano, "Lyapunov vector fields for autonomous unmanned aircraft flight control," *J. Guid. Control Dynam.*, vol. 31, no. 5, pp. 1220-1229, 2008.

[54] E. W. Frew, D. A. Lawrence, and S. Morris, "Coordinated standoff tracking of moving targets using Lyapunov guidance vector fields," *J. Guid. Control Dynam.*, vol. 31, no. 2, pp. 290-306, 2008.

[55] S. Yoon, S. Park, and Y. Kim, "Circular motion guidance law for coordinated standoff tracking of a moving target," *IEEE Trans. Aerosp. Electron. Syst.*, vol. 49, no. 4, pp. 2440-2462, 2013.

[56] V. M. Goncalves, L. C. Pimenta, C. Maia, B. C. Dutra, and G. A. Pereira, "Vector fields for robot navigation along time-varying curves in *n*-dimensions," *IEEE Trans. Robot.*, vol. 26, no. 4, pp. 647-659, 2010.

[57] T. H. Kim and T. Sugie, "Cooperative control for target-capturing task based on a cyclic pursuit strategy," *Automatica*, vol. 43, no. 8, pp. 1426-1431, 2007.

[58] J. L. Ramirez-Riberos, M. Pavone, E. Frazzoli, and D. W. Miller, "Distributed control of spacecraft formations via cyclic pursuit: theory and experiments," *J. Guid. Control Dynam.*, vol. 33, no. 5, pp. 1655-1669, 2010.

[59] A. Franchi, P. Stegagno, and G. Oriolo, "Decentralized multi-robot encirclement of a 3D target with guaranteed collision avoidance," *Auton. Robot.*, vol. 40, no. 2, pp. 245-265, 2016.

[60] Z. Miao, D. Thakur, R. S. Erwin, J. Pierre, Y. Wang, and R. Fierro, "Orthogonal vector field-based control for a multi-robot system circumnavigating amoving target in 3D," *Proc. of IEEE Conf. Decision Control*, pp. 6004-6009, 2015.

[61] H. Lutkepohl, *Handbook of Matrices*, John Wiley and Sons, New York, 1997.

[62] J. Stewart, *Multivariable Calculus*, Cengage Learning, Belmont, CA, 2011.

Hang Zhong received the M.S. and B.S. degrees in automation from the College of Electrical and Information Engineering, Hunan University, Changsha, China, in 2013 and 2016, respectively. He is currently pursuing a Ph.D. degree in control theory and application also in Hunan University. His current research interests include robotics modeling and control, visual servo control and path planning of the aerial robots.

Yaonan Wang received the Ph.D. degree in electrical engineering from Hunan University, Changsha, China, in 1994. He was a Post-Doctoral Research Fellow with the Normal University of Defence Technology, Changsha, from 1994 to 1995. From 1998 to 2000, he was a Senior Humboldt Fellow in Germany, and, from 2001 to 2004, he was a Visiting Professor with the University of Bremen, Bremen, Germany. Since 1995, he has been a Professor with the College of Electrical and Information Engineering, Hunan University. His current research interests include robotics and image processing.

Zhiqiang Miao received the B.S. and Ph.D. degrees in electrical and information engineering from Hunan University, Changsha, China, in 2010 and 2016, respectively. From 2016 to 2018, he was a post-doc fellow with The Chinese University of Hong Kong, Hong Kong. Now, he is an Associated Professor with the College of Electrical and Information Engineering, Hunan University. His research interests include multi-robot systems, cooperative control, and nonlinear system and control.

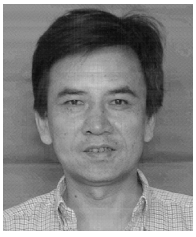

Jianhao Tan received his B.S. degree in the Forging Equipment and Engineering from Huazhong Technology College, Wuhan, China, in 1983, and an M.S. degree in the Pressure Process from Huazhong University of Engineering and Technology, Wuhan, China, in 1989, and a Ph.D. degree in Control Science and Engineering from Hunan University, Changsha, China, in 2010. In 1989, He joined the College of Electrical and Infomation Engineering, Hunan University. He research interests include data mining, pattern recognition, system identification, and image processing.

Ling Li received the B.S. and M.S. degrees in Electronic Science and Technology from the College of Electrical and Information Engineering, Hunan University, Changsha, China, in 2014 and 2017, respectively. She joined the College of Electrical and Infomation Engineering, Changsha University of Science and Technology, Changsha, China. Her current research interests include embedded system design and visual servo control of the robots.

Hui Zhang received the B.S., M.S., and Ph.D. degrees in pattern recognition and intelligent system from Hunan University, Changsha, China, in 2004, 2007, and 2012, respectively. He is currently an Assistant Professor with the College of Electrical and Information Engineering, Changsha University of Science and Technology, Changsha, China. His research interests include machine vision and visual detection.

Rafael Fierro received the M.Sc. degree in control engineering from the University of Bradford, Bradford, UK, in 1990, and the Ph.D. degree in electrical engineering from the University of Texas at Arlington, in 1997. He is currently a Professor of the Department of Electrical Computer Engineering, University of New Mexico (UNM) where he has been since 2007. Prior to joining UNM, he held a postdoctoral appointment with the GRASP Laboratory at the University of Pennsylvania and a faculty position with the Department of Electrical and Computer Engineering at Oklahoma State University. His research interests include hybrid and embedded systems, heterogeneous multivehicle coordination, cooperative and distributed control of multi-agent systems, mobile sensor networks, and robotics. He directs the Multi-Agent, Robotics, Hybrid and Embedded Systems Laboratory at UNM. Dr. Fierro was the recipient of a Fulbright Scholarship, a 2004 National Science Foundation CAREER Award, and the 2007 International Society of Automation Transactions Best Paper Award. He is serving as associate editor for the Journal of Intelligent and Robotics Systems, IEEE Control Systems Magazine, and IEEE Transactions on Automation Science and Engineering.